# Characterization of TiS$_2$ composite cathodes with solid polymer electrolyte

Seong-In Moon [a,*], Jong-Uk Kim [a], Bong-Soo Jin [a], Yoo-Eup Hyung [a], Mun-Soo Yun [a], Hal-Bon Gu [b], Yo Ko [c]

[a] Battery Technology Team, Korea Electrotechnology Research Institute, 28-1 Sungju-dong, Changwon, Kyungnam 641-600, South Korea
[b] Department of Electrical Engineering, Chonnam National University, 300 Yongbong-dong, Kwangju 500-757, South Korea
[c] R&D Management Center for Energy and Resources, 935-34, Pangbae-dong, Seocho-ku, Seoul 137-060, South Korea

## Abstract

A TiS$_2$ composite cathode for lithium polymer battery was developed. We investigated the a.c. impedance response as a function of temperature and charge/discharge cycling process and charge/discharge characteristics of TiS$_2$ composite/solid polymer electrolyte/Li cells. The passivation layer resistance of the Li/solid polymer electrolyte interface at 25 °C was 292 $\Omega$ cm$^2$. The total resistance of the TiS$_2$ bulk and the TiS$_2$/solid polymer electrolyte interfaces was 96 $\Omega$ cm$^2$ The cell resistance significantly decreased at 60 °C. The discharge capacity of the TiS$_2$ composite cathode with 40 wt.% solid polymer elctrolyte was 173 and 146 mAh/g based on TiS$_2$ at cycle nos. 1 and 20 at 25 °C, respectively. The utilization TiS$_2$ at the discharge processes nos. 1 and 20 at 25 °C were 72 and 61%, respectively. TiS$_2$ composite cathode with 40 wt.% solid polymer electrolyte showed better capacity with cycling. © 1997 Published by Elsevier Science S.A.

## 1. Introduction

Titanium sulfide (TiS$_2$) is known to be one of the cathode materials for use in rechargeable lithium batteries [1–3]. Polymer electrolytes were discovered by Fenton et al. [4] in 1973. Wright [5] reported that complexes formed with poly(ethylene oxide) (PEO) and alkali metal salts exhibited high ionic conductivity. Subsequently, these complexes were proposed by Armand et al. [6] as a polymer electrolyte for solid-state battery and electrochemical device applications. Polymer electrolyte provided the interesting possibility of developing lithium polymer battery (LPB) [7]. Croce and Scrosati [8] reported that a passivation film grew rapidly on the lithium surface. In general, cathodes consist of active material, an electron conductor such as acetylene black and a binder. However, the composite cathode for LPB needs an additional amount of solid polymer electrolyte (SPE) in order to improve the lithium ionic conductivity in the cathode. Especially, a good performance of charge/discharge cycling in LPB requires an optimal composition of the composite cathode in LPB.

In this study, we investigated the charge/discharge characteristics as a function of the temperature and the SPE content in TiS$_2$ composite cathode material.

## 2. Experimental

High molecular weight PEO (mol. wt. $2 \times 10^6$), LiClO$_4$, acetonitrile, propylene carbonate (PC), ethylene carbonate (EC) and zeolite were supplied by Aldrich. Zeolite with a mean particle size of 2.5 μm was dried overnight at 200 °C under vacuum. LiClO$_4$ and PEO were dissolved in acetonitrile, the ratio of EO/Li was 8 (EO represents repeating unit of PEO), and PC, EC and zeolite were added. The solution was homogeneously mixed. The polymer electrolyte films were prepared by solution casting. After the evaporation of the solvent the electrolyte films were vacuum dried at 50 °C for 12 h, yielding films of 100 μm thickness.

The composite cathode slurry was prepared by mixing TiS$_2$ powder (< 1 μm) with acetylene black and SPE solution without zeolite. We prepared the TiS$_2$ composite films with three different SPE levels: 30 wt.% (A cell), 40 wt.% (B cell) and 50 wt.% (C cell). The slurry was stirred for 3 h. The composite cathode films were prepared by coating the

slurry on an aluminum foil current collector. After solvent evaporation, the composite films were vacuum-dried at 50 °C for 6 h. The thickness of $TiS_2$ composite cathode films was 30 μm.

The $TiS_2$/SPE/Li cells were constructed from laminates of three types of $TiS_2$ composite cathode, electrolyte film and lithium metal foil. The area of $TiS_2$/SPE/Li cells were 2 cm × 2 cm. The constant current charge/discharge cycling of $TiS_2$/SPE/Li cells was carried out using a battery tester (Maccor). The current density during charge/discharge was 0.02 and 0.1 mA/cm² at 25 and 60 °C, respectively. A.c. impedance analysis (IM6 impedance measurement system, Zahner Electrik) was carried out to measure the variation of the cell resistance as a function of the charge/discharge cycling. The a.c. signal was applied across the cells and its frequency range was from 50 mHz to 2 MHz. All preparation and a.c. impedance and charge/discharge tests of the electrolyte films were carried out in an argon-filled dry box controlled under a water vapor of less than 10 ppm.

## 3. Results and discussion

Typical a.c. impedance spectra of SUS/SPE/SUS, Li/SPE/Li and $TiS_2$/SPE/Li cells at 25 and 60 °C are shown Fig. 1. The a.c. impedance response of SUS/SPE/SUS cell exhibited a capacitive behavior due to the SPE bulk resistance SUS/SPE/SUS interfacial capacitance. From the impedance spectra of three cells in Fig. 1, the bulk resistance of the SPE electrolyte was 2.9 and 1.9 Ω at 25 and 60 °C, respectively. The impedance spectrum of $TiS_2$/SPE/Li cell consists of a semicircle in the frequency range of 35 kHz–2 Hz and a line inclined to the real axis in the frequency range of 2 Hz–0.05 Hz at 25 °C. The semicircle can be interpreted as a result of the charge-transfer process and the composite resistance in the $TiS_2$ composite cathode and the passivation layer on the lithium electrode. This semicircle was smaller at 60 °C than that of at 25 °C.

The equivalent circuit representing the a.c. response of $TiS_2$/SPE/Li cell is given Fig. 2. The mobility of the lithium ion in the polymer electrolyte is dominated by the resistor,

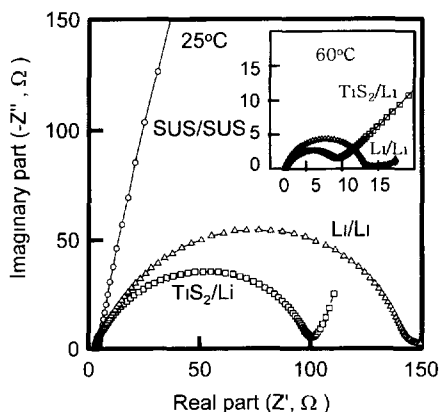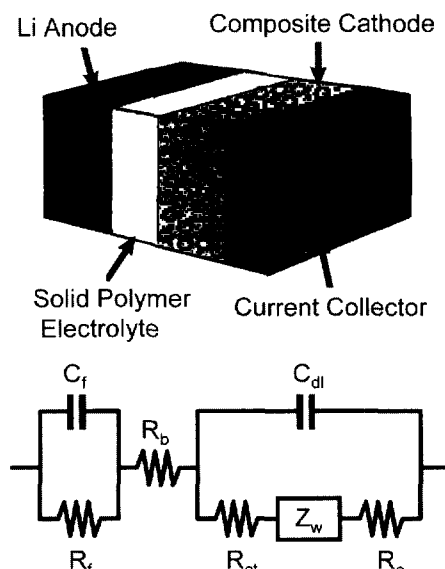Fig. 2. Equivalent circuit of $TiS_2$/PEO–LiClO$_4$–PC–EC/Li cell

$R_b$. The equivalent circuit of the Li/SPE interface is represented by parallel combination of the passivation layer resistance $(R_f)$ and capacitance $(C_f)$. The equivalent circuit elements of $TiS_2$/SPE consist of a charge-transfer resistance $(R_{ct})$ for the $Li^+$ ion intercalation process, $TiS_2$ composite resistance $(R_e)$, double-layer capacitance $(C_{dl})$ and Warburg impedance resulting mass transport in $TiS_2$ particles. We defined the $TiS_2$ composite resistance $(R_e)$ and the charge-transfer resistance $(R_{ct})$ as the cathode resistance.

Fig. 3 shows the comparison of the resistance of various components and interfaces at 25 and 60 °C. The resistance of the Li/SPE/Li cell was 596 and 55 Ω cm² at 25 and 60 °C, respectively. On the other hand, the resistance of the $TiS_2$/SPE/Li cell was 400 and 36.9 Ω cm² at 25 and 60 °C, respectively. We calculated the resistance of the components and interfaces from a.c. impedance spectra in Fig. 1. The passivation layer resistance of the Li/SPE interface was 292 Ω cm² at 25 °C. The total resistance of the $TiS_2$ bulk and $TiS_2$/

Fig. 1. Impedance plot of three types of cell at 25 and 60 °C.

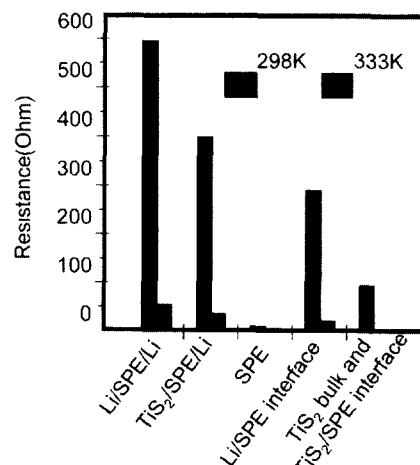Fig. 3. Comparison of the resistance of various components and interfaces at 25 and 60 °C

SPE interfaces was 96 $\Omega$ cm$^2$. On the other hand, the cell resistance was significantly decreased at 60 °C The resistance of the passivation layer was 23.7 $\Omega$ cm$^2$ and the resistance of the TiS$_2$ bulk and TiS$_2$/SPE interfaces was 5.3 $\Omega$ cm$^2$ at 60 °C. The SPE bulk resistance was absolutely small, comparing with the interface resistances and the variation of the bulk resistance was very small between 25 and 60 °C, but the interface resistances were significantly changed. It revealed that the total resistance of the TiS$_2$/SPE/Li cell mainly depended on resistance of the passivation layer formed on the lithium electrode.

Fig. 4 shows the impedance plot of TiS$_2$/SPE/Li cell as a function of charge/discharge cycling at 25 °C, showing that the radius of the semicircle is associated with the interfacial resistance and that the cathode resistance of the TiS$_2$/SPE/Li cell did not change from the initial state until the third cycle. The cell resistance was 90 and 93 $\Omega$ at the initial state and third discharge, respectively. After that the cell resistance increased with increasing charge/discharge cycle number. On the other hand, as shown in Fig. 5, the increase in cell resistance was small during charge/discharge cycling at 60 °C. We guess that the increase in cell resistance is attributed to the increment of the passivation layer resistance.

The specific capacity of the TiS$_2$ composite cathode as a function of the SPE content in TiS$_2$ composite cathodes is
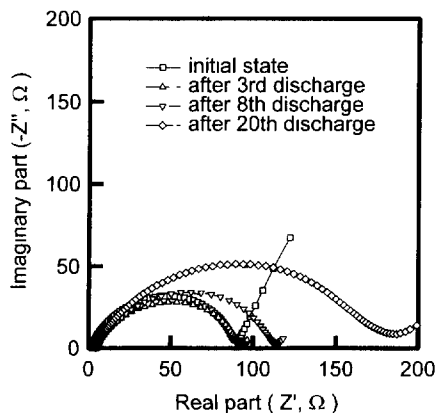


Fig. 4. Impedance plot of TiS$_2$/PEO–LiClO$_4$–EC/Li cell as a function of charge/discharge cycling at 25 °C (A cell) cell area: 2 cm × 2 cm.
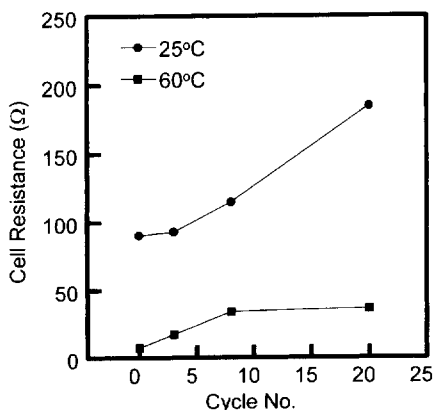


Fig 5 Comparison of the resistance of TiS$_2$/PEO–LiClO$_4$–PC–EC/Li cell as a function of charge/discharge cycling at 25 and 60 °C.



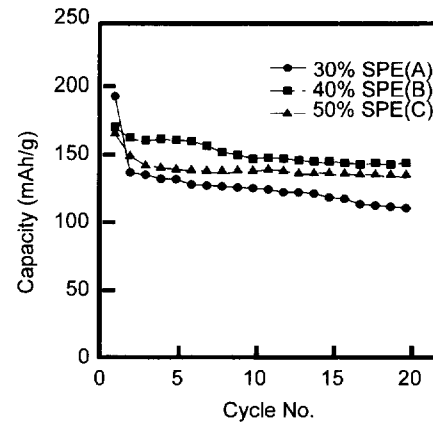Fig. 6. Discharge capacity of TiS$_2$/PEO–LiClO$_4$–PC–EC/Li cell as a function of SPE content at 25 °C; current density: 0 02 mA/cm$^2$, and voltage range: 1.6–2.6 V.

shown in Fig. 6. The theoretical capacity of TiS$_2$ calculated from Li$_x$TiS$_2$ ($0 < x < 1$) is 239 mAh/g. The discharge capacity based on TiS$_2$ of the A cell (TiS$_2$ composite with 30 wt.% SPE) was 196 and 112 mAh/g at cycle nos. 1 and 20 at 25 °C, respectively. This difference of the discharge capacity was nearly 40%. However, fading in capacity of B cell (TiS$_2$ composite with 40 wt.% SPE) and C cell (TiS$_2$ composite with 50 wt.% SPE) was lower than that of A cell. The discharge capacity based on TiS$_2$ of the B cell was 173 and 146 mAh/g at cycle nos. 1 and 20, respectively. The utilization based on TiS$_2$ at the discharge processes nos. 1 and 20 were 72 and 61%, respectively. The Ah efficiency was above 95% at all cycles.

Fig. 7 shows the change in capacity and cell resistance of three types of TiS$_2$/SPE/Li cell using the TiS$_2$ composite cathode at 25 °C. Comparison of the cell resistance of the A, B and C cells at cycle nos. 1 and 20 revealed that the resistance of A cell became higher than that of B and C cells because of a lower SPE content in the TiS$_2$ composite cathode. Moreover, at the 20th cycle, the resistance of A cell was seriously increased compared with its original resistance. In case of the B and C cells, however, the increment of the cell resistance
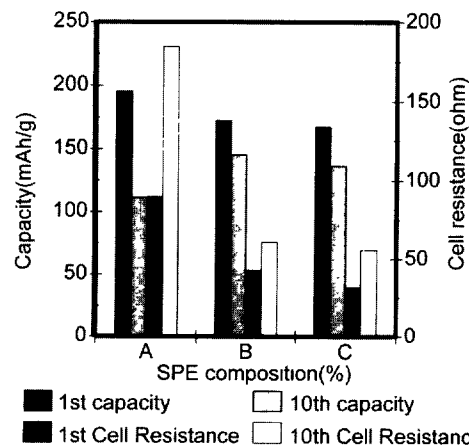


Fig. 7. Charge of capacity and cell resistance of three types of TiS$_2$/SPE/ Li cell TiS$_2$ composite cathode at 25 °C.
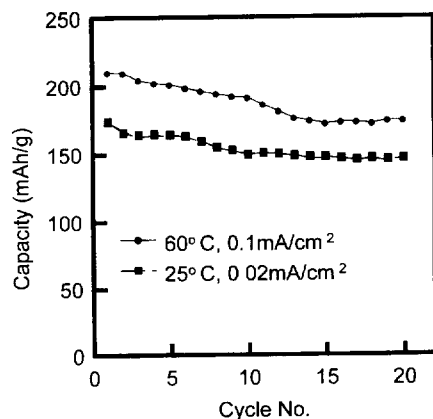
Fig. 8. Discharge capacity of $TiS_2$/PEO–LiClO$_4$–PC–EC/Li cells at 25 and 60 °C; voltage range 1 6–2.6 V

with charge/discharge cycling was not so high. We considered that the capacity fading during charge/discharge cycling is due to the increment of the cell resistance and that it is affected by the preparation conditions of the $TiS_2$ composite cathode with SPE.

Fig. 8 exhibits the specific capacity of B cell at 25 and 60 °C, respectively. The discharge capacity of B cell was 210 and 174 mAh/g at the first and 20th cycles at 60 °C, respectively. The utilization at the first and 20th discharge processes were 87 and 72% at 60 °C, respectively. From these results, we can insist that the $TiS_2$ composite cathode with 40 wt.% SPE content showed better capacity with cycling.

## 4. Conclusions

The passivation layer resistance of the Li/SPE interface was 292 $\Omega$ cm$^2$ at 25 °C. The total resistance of the $TiS_2$ bulk and $TiS_2$/SPE interfaces was 96 $\Omega$ cm$^2$. On the other hand, the cell resistance was significantly decreased at 60 °C. The increase in cell resistance is attributed to the increment of the passivation layer resistance. The discharge capacity of the B cell was 173 and 146 mAh/g at cycle nos. 1 and 20, respectively. The utilization at discharge processes nos. 1 and 20 were 72 and 61%, respectively. The Ah efficiency was above 95% at all cycles. The $TiS_2$ composite cathode with 40 wt.% SPE content showed better capacity with cycling.

## References

[1] M S Whittingham and F.R. Gamble, Mater Res. Bull, 10 (1975) 363.

[2] M S Whittingham, Prog. Solid State Chem., 12 (1978) 41.

[3] T Uchida, K. Kohiro, H. Hinode, M. Wakihara and M Taniguchi, Mater. Res. Bull., 22 (1978) 935.

[4] B.E. Fenton, J.M. Parker and P V. Wright, Polymer, 14 (1973) 589

[5] P.V Wright, Br Polymer J, 7 (1975) 319

[6] M.B. Armand, J.M. Chabagno and M.J. Duclot, 2nd Int. Meet. Solid Electrolytes, St Andrew, Scotland, UK, 1978, p 20

[7] K M Abraham and M. Alamgir, J. Power Sources, 43–44 (1993) 195

[8] F. Croce and B Scrosati, J. Power Sources, 43–44 (1993) 9.